1-1-2014

Determination Of Jet Transport Parameters And Their Temperature Dependence In Heavy-Ion Collisions

Karen Marie Burke
Wayne State University,

DETERMINATION OF JET TRANSPORT PARAMETERS AND THEIR TEMPERATURE DEPENDENCE IN HEAVY-ION COLLISIONS

by

KAREN MARIE BURKE

THESIS

Submitted to the Graduate School

of Wayne State University,

Detroit, Michigan,

in partial fulfillment of the requirements

for the degree of

MASTER OF SCIENCE

2014

MAJOR: PHYSICS

Approved By:

_____

Advisor Date

DEDICATION

To Mom, Dad, Jonathan, Uncle Johnny, and Benjamin -

thank you for believing in me even when I didn't.

ACKNOWLEDGEMENTS

I would like to thank: Dr. Abhijit Majumder for his guidance in my research and his support of my educational goals. Dr. Rosi Reed for her willingness to participate in my thesis defense as a member of my committee. Dr. Sean Gavin for participating in my thesis defense as a committee member and his guidance during my studies at Wayne State University. Dr. Ratna Naik and Dr. Joseph Dunbar for taking time from their busy schedules to write letters to help obtain the funding necessary to complete this work. My friends and fellow students - Michael Kordell, Christopher Zin, Derek Everett, and Jacob Elledge for assisting with my thesis preparation. My parents (Art and Karen Burke) and brother (Jonathan Burke) for believing in me and standing by me. Alysse Reynolds for her constant encouragement. Wissam Fawaz for helping me stay on track. Ben Seligson for being understanding and helping me through this process.

TABLE OF CONTENTS

LIST OF FIGURES

CHAPTER 1: INTRODUCTION AND GOALS

Jets have been found to play an integral role in the study of the quark gluon plasma (QGP). From the time they are created in high energy nuclear collisions to the moment they exit the QGP and hadronize, they are influenced by the medium through which they propagate, and thus their modification carries evidence about properties of the QGP. Through perturbative quantum chromodynamics (pQCD), the initial rate of jet production can be calculated, and from there analysis of jet energy loss and suppression of final jets due to interaction with the medium can be done. The first theoretical studies done using this method [1-17], combined with research on hard probes in vacuum were the foundation of experimental studies at the Relativistic Heavy-Ion Collider (RHIC) as well as the phenomenological studies that resulted.

The research teams at RHIC have proven its usefulness in providing insight into high energy nuclear physics. Since its inception, RHIC has supplied supporting data for jet quenching phenomena such as single inclusive hadron spectra at large transverse momentum (p_T) [18, 19], back-to-back high p_T dihadron correlations [20] and back-to-back γ-hadron correlations [21-23]. Recently, the Large Hadron Collider (LHC) has provided even more support in these areas [24-26]. RHIC has also produced supporting evidence of reconstructed jet supression [27-29], increased dijet symmetry [30, 31], and increased γ-jet asymmetry [32, 33]. Though several models [34-46] for jet quenching and parton energy loss have been used in the studies at RHIC, in this thesis I will focus solely on the higher twist (HT) method of investigating parton energy loss in dense matter as jets propagate through the QGP. Some of these models have been supported [47-50] by experimental data from the more recently studied LHC data, and some have been found to have discrepancies [24, 25, 51]. The resultant data pool of jet quenching data

from both RHIC and the LHC have nonetheless provided new constraints on medium properties in even the best experimentally supported models.

A goal of heavy ion collision studies is to use phenomenological studies of experimental data from RHIC and the LHC combined to extract properties of the QGP medium for a variety of jet quenching measurements. For my part in this goal, I have carried out a study of medium properties as they apply to the higher twist model, using large p_T single inclusive hadron spectra suppression data from experiments. The only property of the medium that affects parton energy loss in the HT approach [49] is the jet transport coefficient $\hat{q}$, a direct fit parameter for parton energy loss. I will use a range of values for $\hat{q}$, which is the average p_T^2 per unit length imparted from a hard parton that propagates without radiation. I will calculate the nuclear modification factor R_{AA} and compare this value to data provided by PHENIX at RHIC, and ALICE and CMS at the LHC. The jet will be assumed to be initiated by a light quark or gluon, which is a constraint that is built in to the code used to calculate my results.

To appropriately study energy loss and medium modification, it is important to include calculations that incorporate dynamic bulk matter evolution [52-54]. In this thesis, a 2+1D ideal (constant rapidity profile - used particularly in my calculations) [55-58] hydrodynamic simulation was used. These simulations provide space-time information on the evolution of the medium, essential in the phenomenological study of jet quenching presented in this thesis. By utilizing experimentally constrained simulations which utilize bulk matter evolutions that have been averaged over several calculations, we are able to get a more accurate picture of the bulk medium evolution. In addition, it shows us details about charged hadron spectra and their azimuthal properties. Another benefit of constraining bulk hadron production in heavy ion collisions is reduced uncertainty in calculations.

My work in this thesis has taken advantage of progress since the initial attempts to extract the jet quenching parameter [53, 54]. These previous efforts resulted in diverging values, which varied by a factor as high as 8. Since then, we have made significant progress in jet quenching studies, particularly in our theoretical understanding and modeling of such phenomena, including how we expect the medium to behave after the initial collision of the heavy ions. In this work, I have used new data from experiments at RHIC and the LHC to restrict my calculations of the jet transport parameters. Temperature and energy dependence have also been investigated, made possible by the large difference of initial temperature and range of p_T attained at the LHC versus that at RHIC.

In the remainder of this thesis, I will briefly review concepts essential to this study, before presenting and discussing results. This goal will be achieved in the following manner: I will begin in Chapter 2 with a discussion of background material. I have included a brief outline of the four known forces in nature, discussions of the quark and parton models, and will close the chapter with a short explanation of deep inelastic scattering (DIS). From there I will continue my outline of the field in Chapter 3 through an elementary discussion of quantum chromodynamics (QCD) and an explanation of what happens in high energy nuclear collisions. The information in Chapter 4 will bring us to the topics of the quark gluon plasma, jets and jet quenching, transport coefficients, and the higher twist model. I will describe the quark gluon plasma and then jets: what they are made of and what we know about how they interact with the QGP medium. The discussion of the HT approach to parton energy loss employed in this work will include an outline of the constraints on the jet transport parameter in the HT model and their investigation by comparing the calculated suppression factors for single hadron spectra with experimental data from RHIC and the LHC. Finally, in Chapter 5, results are compiled with

these constraints to provide an up-to-date estimate of the jet transport parameter and its temperature dependence within the range that has been reached in the most central Au+Au collisions at RHIC and Pb+Pb collisions at the LHC.

CHAPTER 2: BACKGROUND

2.1 Known Forces in Our Universe

Our current understanding of the universe accounts for four known forces in nature: gravity, the electromagnetic force, the weak nuclear force, and the strong nuclear force. The force of gravity is the force that governs our "classical" world. This interaction between macroscopic bodies like Earth and the Moon, or even two objects as small as marbles resting on a desk, constitutes gravitational physics we can see in everyday life. The second force is the electromagnetic force. This is the force that exists due to the interactions between charges and currents. We recognize this force when we perform simple experiments like placing a magnet near iron filings. Next there is the weak nuclear force. This force has been proven to exist through our experimental and theoretical studies of nuclear (radioactive) decay. Finally we come to the strong nuclear force, which is the force being studied in this thesis. This is the force that holds together the fundamental particles that comprise nucleons and other particles bound by the strong force; a residual strong force holds nucleons within nuclei. The work in this thesis has been done to contribute to the advancement of our knowledge and understanding of the strong force.

2.2 The Quark Model

In the 1950s, it was determined that protons and neutrons are not fundamental particles, different from the electron, which is a fundamental particle. Protons and neutrons are made up of smaller particles known as quarks, anti-quarks, and gluons. These particles make up not only protons and neutrons but also all other strongly interacting particles that exist and interact with

each other within the domain of the strong force. Quarks and anti-quarks have typical properties of matter like mass and electric charge, however they also have flavor and color charge [59].

Quarks are fermions, which means that in addition to being fundamental particles, they carry spin 1/2, like leptons, and follow the Pauli exclusion principle. Quarks have 6 flavors: up, down, strange, charmed, top, and bottom. At the time of this writing, quarks and anti-quarks have never been found in free stable states. Quarks carry electric charge as wells as color charge. Up, charmed, and top quarks carry the charge +2/3e, while down, strange, and bottom quarks carry an electric charge of -1/3e, where e is the magnitude of the charge of the electron (or proton): $e = 1.602176 \times 10^{-19}$C. Each quark also has a respective anti-quark, which has "opposite" or anti-color charge (discussed below) and opposite electric charge.

Within the quark model, Gell-Mann gave a description of constituent quarks [60]. In low energy regimes, only three quarks are visible within a nucleon. In the case of the proton, this corresponds to two up and one down. While the color of each up or down quark is not relevant, it is essential that each of the three colors (red, blue, green) are present within each nucleon. Gell-Mann's model was immediately shown to be successful within the range of low energy studies, allowing a number of "new" strongly interacting particles to be discovered. [59]

2.3 The Parton Model

Another model used to describe the structure of hadrons such as the proton is the parton model. Unlike the quark model, the parton model includes a description of gluons as well as quarks. The term parton generally refers to quarks, anti-quarks, and gluons that have been boosted, and thus have high energy and momentum.

Gluons carry a spin of 1 and are massless. Similar to photons, they are the initiators of interaction between particles, in this case quarks and anti-quarks [59, 61]. Due to their lack of charge, photons are unable to interact with themselves. While gluons carry no electric charge, they do have color charge. Since they have color charge they can, unlike photons, interact with themselves as well as quarks, anti-quarks, and other gluons.

Within the parton model description of hadrons, there are two types of quarks: sea, and valence. Valence quarks carry the net flavors of the hadron, for example the case of the proton, there are two excess flavor up quarks and one excess flavor down quark. These tend to have non-negligible support at larger momentum fractions of the hadron. The sea quarks and anti-quarks represent all other flavor carrying partons in the hadron whose net flavor is always vanishing. These tend to have greater support at smaller momentum fractions of the nucleon. The sea quarks are the quarks and anti-quarks that generally become the quark gluon plasma upon collision of two heavy nuclei. On occasion, sea quarks can participate in hard scattering, but rarely become jets as the result of a collision. The number of valence quarks in the nucleon is always fixed, however the number of sea quarks will depend on the resolution of the probe. Net flavor in the sea quark plus sea anti-quark population always zero.

In the parton model, each hadron traveling at high momentum is composed of several almost non-interacting partons which carry different fractions of the momenta of the parent hadron. We artificially divide these into two "types" of partons: soft and hard. The term "soft" refers to the partons that have a lower momentum, and therefore lower frequency. These partons, which have a momentum ratio of $p_{parton}/p_{proton} <<<1$, are the particles that provide the soft interactions that mainly create the quark gluon plasma (QGP), a very hot, dense matter thought to be created from these high energy collisions. The hard partons have a momentum

ratio of momentum ratio of $p_{parton}/p_{proton} \leq 1$, and generally are the partons that form jets upon interaction with other hard quarks, anti-quarks, and gluons during nuclear collisions. These jets are then used as probes to investigate the properties of the QGP .

2.4 Deep Inelastic Scattering

Increasing the momentum of an electron effectively increases the frequencies associated with its wave function. Using this property, it is possible to bombard a stationary proton with such an electron to examine the "contents" of the proton. During this process, other hadrons and strongly interacting particles were found to be broken off from the proton due to the high energy scattering of the impacting electron. This observation in Deep-Inelastic Scattering (DIS) experiments led to the discovery of quarks. At higher momentum exchange and energy of the electron, it was found that the proton was composed of many more than 3 objects. The results of DIS experiments could be described assuming that the partons were traveling as almost free particles within the high energy nucleon. This inelastic scattering of an electron off a constituent particle within the proton proved there were three point-like particles within a proton [62, 63].

CHAPTER 3: HOT STRONGLY INTERACTING MATERIAL

3.1 Quantum Chromodynamics

Quantum Chromodynamics (QCD) is the theory of strong interactions of particles which involves interaction due to color charge. To gain an initial, elementary understanding of these interactions, we can draw some parallels between color interactions and the electrostatic interactions of electrically charged particles. Introductory electrostatics tells us that the interaction created by the electrostatic force will cause two particles with opposite charges to attract each other, and like charges to repel each other. In addition to the attractive force that is observed when two oppositely charged particles are placed near each other, we also know that particles such as an electron ($e^- = -1.602x10^{-19}$) and a positron ($e^+ = 1.602x10^{-19}$) create a dipole when placed near each other. When viewed from far away, the effects of the dipole cause the system to appear neutrally charged. Finally, we consider the effect an electrically charged particle has on a dielectric. We know that the charged particle will polarize the dielectric, and thus the dielectric will have a shielding effect on the charge. Therefore, from a distance it will seem as though the charge is actually smaller than it is in reality. The consequence of this is that we are only able to see larger net charge at very large momentum transfer.

Since quarks and anti-quarks have electric charge, they will interact according to the rules of electromagnetism; more importantly for the scope of this thesis, due to their color charge, they will interact through the strong force [61]. In QCD, there are three possible color charges for quarks, and three opposite color charges, or anti-colors, for anti-quarks. Due to the interaction created by the strong force, quarks with like colors will repel each other, and those with different, as well as opposite color and anti-color will attract each other. Quarks have been given the color charge designations of red (R), blue (B), and green (G), whereas anti-quarks are labeled

as anti-red ($\overline{R}$), anti-blue ($\overline{B}$), and anti-green ($\overline{G}$) [62]. A quark and its anti-quark placed near each other will produce a dipole of sorts, which causes it to seem like there is no charge present when the pair is observed from a distance. There is a caveat to this, however: when viewed from far away, whether or not the colors "negate" each other depends on the particular color of each quark and anti-quark pair. For example, the color charges of a green quark and an anti-red anti-quark will not look as if there is no charge as would a negative and positive charge. However if there is a pair consisting of a green quark and an anti-quark that is anti-green, the colors will indeed cancel each other's visibility when viewed from far away. In addition to combining color and anti-color to achieve neutrality due to being a dipole viewed from a distance, color neutrality can also be reached through combination of a red, blue, and green quark, as well as a combination of anti-red, anti-blue, and anti-green. Due to the interaction created by the strong force, quarks with like colors will repel each other, and those with opposite color and anti-color will attract each other. For two quarks with different colors, the force may be attractive or repulsive depending on the particular color channel.

Color charge also has important physical consequences when a parton carrying a non-neutral color charge passes through matter. Given a particle with a color charge, there is an entirely different effect as compared to the situation in electromagnetism. When a color charged particle is moving through a medium, it will attract particles of opposite color charge and repel particles of similar charge, thereby polarizing the medium. This however, is where the similarity ends. This color charged particle can also radiate color charge carrying gluons, thereby depleting its own charge and spreading it over the medium. In fact, due to this, the particle actually becomes anti-screened, and so appears to have a smaller charge when probed at very small distances [59]. From this we realize that at large momentum transfer, we penetrate the cloud of

gluons surrounding the elementary color charge, reducing the effectiveness of the interactions of the strong force. This means that when the nuclei are sped up to high momentum, at speeds near the speed of light, some of the valence quarks and anti-quarks within the hadrons that comprise the nuclei basically exist as free pairs of quarks and anti-quarks. While the total color charge will still be neutral for the whole system, this will allow freedom for the valence quarks and anti-quarks to interact upon collision of the two nuclei. The implications of this are huge, and drive the fields of high energy nuclear physics and high energy particle physics. [59]

3.2 High Energy Nuclear Collisions

High energy nuclear collisions are the interactions of heavy-ions (nuclei with their electron clouds stripped off) with other heavy ions or particles like protons and deuterons. These nuclei and particles are sped up in particle accelerators, such as the Relativistic Heavy-Ion Collider (RHIC) at Brookhaven National Lab, and the Large Hadron Collider (LHC) at CERN, to speeds near the speed of light. The results presented in this paper will look particularly at Au+Au and Pb+Pb collisions, as they pertain to experimental data collected in the experiments ALICE (LHC), CMS (LHC), and PHENIX (RHIC). The accelerated nuclei have energies ranging from 200GeV/n at RHIC, to 2.76TeV/n at the LHC, where n is a nucleon pair [64]. This energy value can also vary somewhat depending on the experiment.

As alluded to above, in the collision of these nuclei, softer partons with larger interaction are stopped and lead to the formation of the Quark Gluon Plasma. This plasma will persist as long as the temperature within it is sufficiently high (leading to larger momentum transfers and thus weaker coupling between particles). Due to the large densities and pressures produced the plasma expands and cools. As the temperature drops, the coupling between the particles

increases and the deconfined state eventually transitions back to a plasma of colorless interacting hadrons. As the system continues to expand and cools, these hadrons ``freeze out" and then free stream to the detectors.

3.3 The Quark Gluon Plasma

The quark-gluon plasma (QGP) is a very hot, dense state of matter created upon collision of two high momentum nuclei, or heavy ions. When the two nuclei and their constituents collide, there is an immense transfer of energy, which creates an intense temperature increase, leading to deconfinement: the appearance of color charge degrees of freedom. It is mainly the soft, low momenta partons that make up this deconfined phase. The effect of deconfinement actually strips individual quarks, anti-quarks and gluons from their parent hadrons, allowing individual quarks and gluons to interact with each other. This concept is similar to the idea of the plasma matter within the sun and other stars. Inside stars, the matter is so dense and hot that electrons are separated from nuclei, and are able to move around freely. Using the knowledge that we have of deconfinement, combined with our ability to create these conditions in the lab, we can use perturbative quantum chromodynamic (pQCD) calculations to describe the effects of color interactions from moving partons on media, and then compare the results of these calculations to experimental data.

CHAPTER 4: JETS, JET QUENCHING, AND TRANSPORT COEFFICIENTS

4.1 Jets and Jet Parameters

Occasionally the hard, high frequency, high momenta partons in the colliding hadrons of the nuclei will scatter elastically off each other, creating jets. A parton that is struck by another parton (quark, anti-quark, or gluon), may impart a high enough energy to radiate gluons, which will then propagate through the medium [63]. As they propagate through the medium, they will interact with other partons, emitting other gluons as well as recombining. This process creates a cone-shaped "shower" of partons, or a jet. The formation of jets is a consequence of a weakening of the strong force at high momentum transfer.

It has been observed at RHIC and the LHC that when these partons are ejected from the collision area as jets, they traverse the QGP medium. As they move through the medium, the partons encounter decreasing medium temperature, and lose momentum due to radiation, collisions with and scattering from other partons. They eventually reach a point where the temperature is low enough that they hadronize. When two hard partons collide, two jets are created and leave the collision area in back-to-back trajectories. Each pair of jets will have a different momentum, and a component of the momentum vector of these particles, the transverse momentum (p_T), is the component that is perpendicular to the path of the nuclei immediately prior to their collision.

The jet transport coefficient $\hat{q}$ is defined as the mean transverse momentum squared per unit length, exchanged between a hard parton and the medium. It is an operator of tensor construct, and has the form

$$\hat{q} = \frac{4\pi C_F \alpha_s}{N_c^2 - 1} \int dy^- \langle F^{ai+}(0) F_i^{a+}(y^-) \rangle \, e^{i\xi p^+ y^-}. \qquad (1)$$

In the previous equation, C_F represents the Casimir of the hard parton, $N_c = 3$ are the number of colors of the quarks, and α_s is the strong coupling constant. Inside the integration over negative light-cone separation y^-, the factors F^{ai+} represent the gluon field strengths experienced by the hard parton as it propagates in the negative light-cone direction. The target is assumed to move along the positive light-cone direction with momentum p^+. This parameter describes jet quenching in high energy nuclear collisions, meaning that $\hat{q}$ controls the radiative energy loss [64]. This energy loss is due to induced gluon bremsstrahlung, caused by the scattering experienced by the partons in the jet shower.

The nuclear modification factor, $R_{AA,}$ is a measure of the suppression of the yield of high p_T hadrons in A-A (nucleus-nucleus) collisions, with respect to the yield of a p-p collision scaled up by the number of binary nucleon-nucleon encounters expected to occur in a heavy-ion collision [65]:

$$R_{AA} = \frac{\frac{dN_{AA}}{dp_T dy}}{\langle N_{bin} \rangle \frac{dN_{PP}}{dp_T dy}}. \qquad (2)$$

The scaling factor N_{bin} is the number of nucleon-nucleon collisions that are expected to occur for a given A-A collision. The nuclear modification factor provides a measure of jet modification as it traverses the QGP. If a heavy ion collision was merely a superposition of nucleon-nucleon collisions, we expect to obtain at high momenta ($p_T > 2$ GeV) an R_{AA} value of approximately 1. Suppression is due to energy loss in the medium created in high energy nuclear collisions. As $\hat{q}$ increases, more energy is radiated, meaning more quarks, anti-quarks and gluons are created in the shower of partons. This change in the jet's composition and participants is called nuclear modification.

4.2 The Higher Twist Model

The HT model was developed [66] from the study of twist corrections to deep inelastic scattering. Twist calculations were initially used to describe the physics of partons undergoing a few scattering in a medium. Later it was discovered that this method could be extended to multiple scattering [66]. Contrary to other energy loss approaches, the HT approach directly calculates the medium modified fragmentation function.

In the higher twist model (HT), pQCD is used to calculate the corrections to a hard process in an expansion in powers of λ/Q, or the twist of a collision. In these cases, we are generally looking at a value for $\lambda^2 Q$ of the order of $\Lambda_{QCD} \approx 200$ MeV, while Q (the virtuality) is of the order of a few GeV. Here λ is a small dimensionless parameter, and Q is the perturbative hard scale, or virtuality of a parton. The short range, high energy applications of pQCD are ideal for these calculations. In this thesis, I look at how higher twist corrections are affected by the medium created due to DIS in high energy collisions [46]. Varying path lengths through the medium results in different variations of jet modification, and suppression of the jet occurs by powers of Q^2. This expansion in inverse powers of the momentum transfer is a result of determination of the gradation of parton matrix values that exist between hadron states [66]. From the hierarchy of the expansion and inclusion of phenomenology of the meduim, the medium modified fragmentation functions can then be derived. This scalable value makes this an integral tool in solution of multiple scattering event problems, as it allows for multi-particle correlation generalizations.

4.2 The Higher Twist Calculation

As explained above, the HT approach [46, 67] is a first order calculation of the correction of a fragmentation function evolution in vacuum. The fragmentation function describes the distribution of hadrons formed in the hadronization of a parton, as a function of the momentum fraction of the parent hadron. My calculation is extended from single scattering to include multiple scattering through modified QCD evolution equations. These modified equations involve multiple scattering for induced gluon emission. This modification to the in vacuum fragmentation function is altered utilizing a vacuum plus medium modified kernel. Factorization [68] is explicitly utilized in this calculation; the initial parton distribution functions are factorized from the hard sattering cross section as well as the final fragmentation function. The equation

$$\frac{d\sigma}{dyd^2p_h} = \int d^2bd^2rT_{AB}(b,r)\int dx_a dx_b G_A(x_a,Q^2)G_B(x_b,Q^2)\frac{d\hat{\sigma}}{d\hat{t}}\frac{\widetilde{D}(z,Q^2)}{\pi z}, \qquad (3)$$

is the definition for the cross section in which hadrons of a particular transverse momentum (p_h) for a specified rapidity interval (y) are produced in the collision of two heavy ions.

In the equation above, $T_{AB}(b,r) = \int dz\,\rho_A\left(z,\vec{r}+\vec{b}/2\right)\int dz'\,\rho_B\,(z',\vec{r}-\vec{b}/2\,)$, is called the thickness function, where nucleus A/B has a nuclear density $\rho_{A/B.}$ $G_A(x_A,Q^2)$ and $G_B(x_B,Q^2)$ are the nuclear parton distribution functions of the participant nuclei, these include any corrections necessary due to parton shadowing. Two contributions are considered within the modified fragmentation function $\widetilde{D}(z,Q^2)$. The first is the vacuum evolution, and is contained in the DGLAP equations

$$\frac{\partial D_q^h(z,Q^2)}{\partial log(Q^2)} = \frac{\alpha_s(Q^2)}{2\pi}\int_z^1 \frac{dy}{y} P_{q\to i}(y) D_i^h\left(\frac{z}{y}, Q^2\right). \qquad (4)$$

The medium modified evolution equation [68] provides the second input to the modified fragmentation function

$$\frac{\partial D_q^h(z,Q^2,q^-)}{\partial \log Q^2} = \frac{\alpha_s}{2\pi}\int_z^1 \frac{dy}{y} \int_{\zeta_i}^{\zeta_f} d\zeta P_{q\to i}(y) K_{q^-,Q^2}(y,\zeta) D_q^h(\frac{z}{y}, \mathrm{Q}^2, \mathrm{q}^-, \mathrm{y}). \qquad (5)$$

In Equations (4) and (5), we note the inclusion of the Altarelli-Parisi splitting function $P_{q\to i}(y)$. The factor $K_{q^-,Q^2}(y,\zeta)$ contains all information on the medium modification, such as the jet transport coefficient and phase factors that take into account contributions from emission amplitude interference. The leading contribution to $K_{q^-,Q^2}(y,\zeta)$ is given as [69]

$$K_{q^-,Q^2}(y,\zeta) = \frac{[\hat{q}_A(\zeta) - (1-y)\,\hat{q}_A/2 + (1+y)^2\hat{q}_F]}{Q^2}\left[2 - 2\cos\frac{Q^2(\zeta-\zeta_i)}{2q^- y(1-y)}\right]. \qquad (6)$$

The jet transport coefficient is represented here in two ways. A quark scattering off a gluon field has a jet transport coefficient represented as $\hat{q}_F$. If instead a hard gluon (either by itself or radiated from a hard quark) were to undergo scattering off the glue field, it would entail a jet transport coefficient represented by $\hat{q}_A$. Both jet transport coefficients are position dependent, and $\hat{q}_A$ (for the gluon) can be expressed [70-72] nearly identical to Equation (1), expect with a substitution $C_F \to C_A$, which simply changes the color factor (Casimir) to that of the gluon instead of a quark. The gluon jet coefficient is related to the jet transport coefficient of the quark by $\hat{q}_F = (C_F/C_A)\,\hat{q}_A$.

In general, $\hat{q}$ is assumed to scale with a fundamental property of the medium. For the HT model used in this thesis, I assume that $\hat{q}$ scales with the entropy density s (the Refs. [55, 72] describe other scaling assumptions made for $\hat{q}$): $\hat{q}(s) = \hat{q}_0$ (s/s_0). At an initial time τ_0, s_0 is the maximum entropy density that can be achieved at the highest energy at RHIC in the center of the most central collisions. At this point, $\hat{q} = \hat{q}_0$, and this is when thermalization occurs within the colliding mass. The entropy density profile is calculated within a (2+1)D viscous hydrodynamic module [73, 74] (designed by a hydro group within the JET Collaboration). The initial conditions for RHIC Au+Au collisions (temperature T_0 = 346 MeV, $\sqrt{s}$ = 200 GeV/n) and LHC Pb+Pb collisions (T_0 = 447, $\sqrt{s}$ = 2.76 TeV/n) are calculated using MC-KLN initial conditions. Next the distance integral $K_{q-,Q2}(y,\zeta)$ is sampled to calculate the hadron spectra in the heavy ion collision. This is done by sampling the integral through the evolving medium over a large number of paths, whose starting points come from the binary collisions profile. After averaging the medium length integral over $K_{q-,Q2}(y,\zeta)$, Equations 2 and 3 are used to calculate the medium modified evolution of the fragmentation function.

The input distribution for both the vacuum evolution equation and the medium evolution equation is a vacuum fragmentation function. This function is at an input scale of $Q_0^2 = p/L$, and evolves from $Q_0^2 = 1$ GeV^2 according to the vacuum evolution equation. The mean escape length of jets with a given energy in the medium (L) can be calculated using the energy p of a parton using the single emission formalism of Guo and Wang [12, 13]. Here $p = p_h/z$ is the transverse momentum of the parton which fragments to a hadron with transverse momentum p_h and momentum fraction z.

The results presented in this thesis are updates of the calculations done in Reference [48]. Since publication of the previously mentioned results, there have been some changes to the

numerical routine which calculates these results. The fluid-dynamical simulations now include a new initial state, which uses an MC-KLN that takes into account new data from the LHC. In addition, these hydrodynamic calculations are now averaged over a large ensemble of fluctuating initial conditions [51, 52]. The numerical routine now also averages over those same fluctuating initial conditions to determine jet origin distributions from the binary collision profile consistently.

The following figures (Figures 1 and 2) compare my calculated values of hadron suppression to experimental data obtained from the PHENIX experiment at RHIC and the experiments CMS and ALICE at the LHC. The experimental data from RHIC is for 0-5% central Au+Au collisions at $\sqrt{s}$ = 200 GeV/n (Figure 1), and the data from the LHC is for 0-5% central Pb+Pb collisions at $\sqrt{s}$ = 2.76 TeV/n) (Figure 2). A range of values for $\hat{q}_0$ was used to obtain values of R_{AA}, which are represented by the lines in the figures. The best fit to experimental data in each plot is illustrated by the solid line. A range of $p_T \geq 5$ and 20 GeV/c were used in the calculations to find the best fit. Finally, Figure 3 presents the χ^2 distributions using the data from Figures 1 and 2. This χ^2 distribution was fit to experimental data and is a function of the initial value of $\hat{q}_{0.}$ The best fit values of the jet transport parameter are $\hat{q}_0$ = 2.0 ± 0.25 GeV2/fm at RHIC and $\hat{q}_0$ = 2.9 ± 0.6 GeV^2/fm at the LHC.

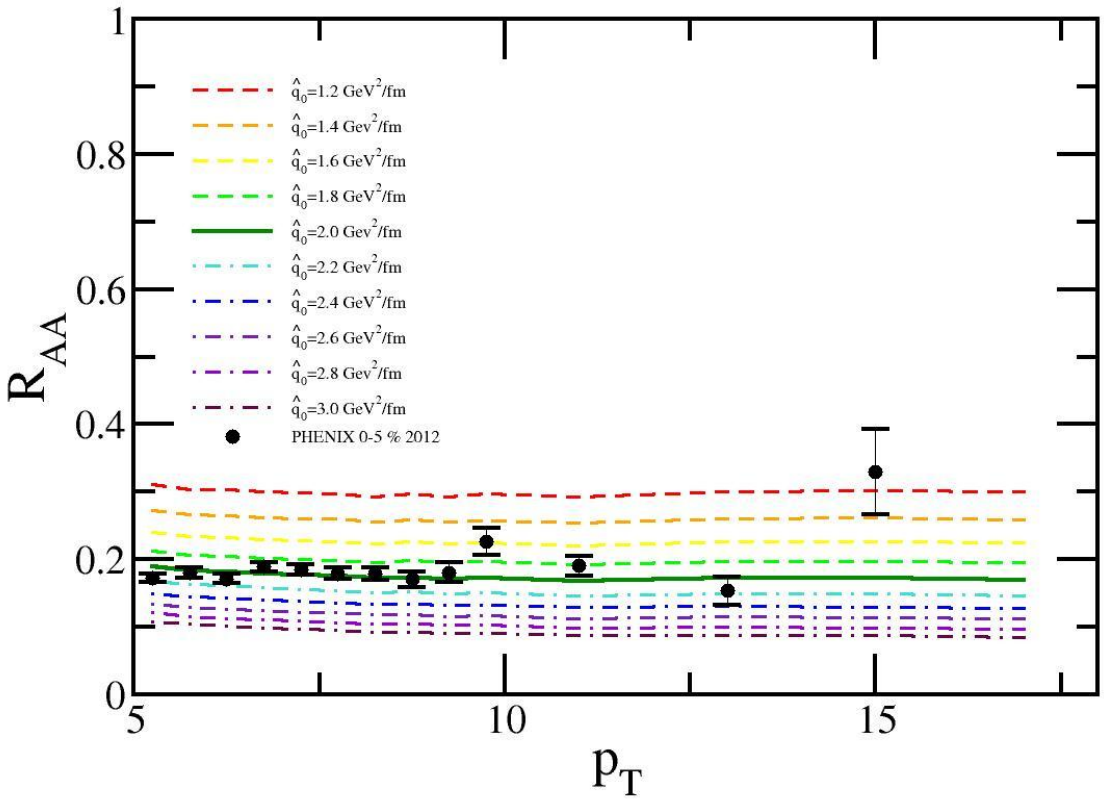

FIGURE 1: R_{AA} Calculated via Higher Twist vs PHENIX (RHIC) data

Results above are for the HT model, as compared to experimental data from RHIC. Mid-rapidity, neutral pion (π^0) spectra, nuclear modification factor R_{AA} values are shown for 0-5% central Au+Au collisions at $\sqrt{s}$ = 200 GeV/n, as they compare to PHENIX [75, 76] (RHIC) data. The hydrodynamics simulation starts at τ_0 =0.6 fm/c, which is when the system thermalizes. At the time of thermalization, initial values of initial gluon jet transport parameter $\hat{q}_0$ range from 1.2-3.0 GeV^2/fm.

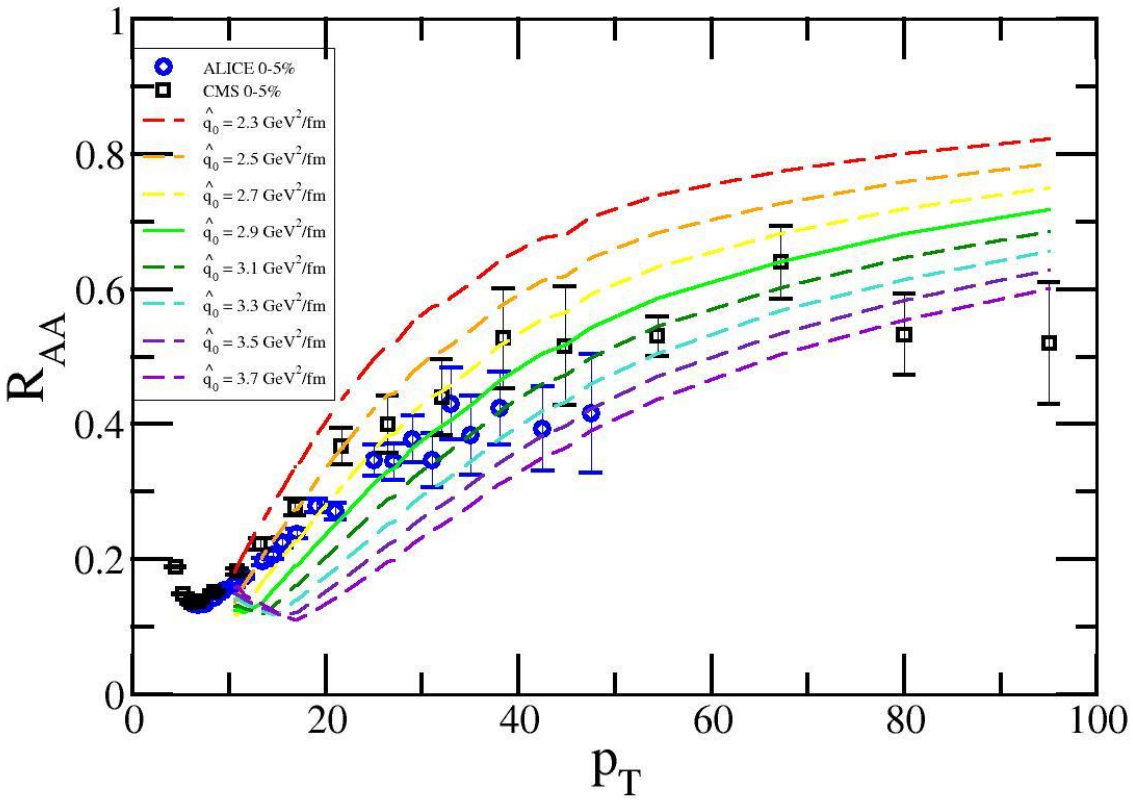

FIGURE 2: RAA Calculated via Higher Twist vs CMS and ALICE (LHC) data

Results above are for the HT model, as compared to experimental data from RHIC. Mid-rapidity, charged particle spectra, nuclear modification factor R_{AA} values are shown for 0-5% central Au+Au collisions at $\sqrt{s}$ = 2.76 TeV/n, as they compare to ALICE [25] and CMS [24] data at the LHC. The hydrodynamics simulation starts at τ_0 =0.6 fm/c, which is when the system thermalizes. At the time of thermalization, initial values of initial gluon jet transport parameter $\hat{q}_0$ range from 2.3-3.8 GeV^2/fm.

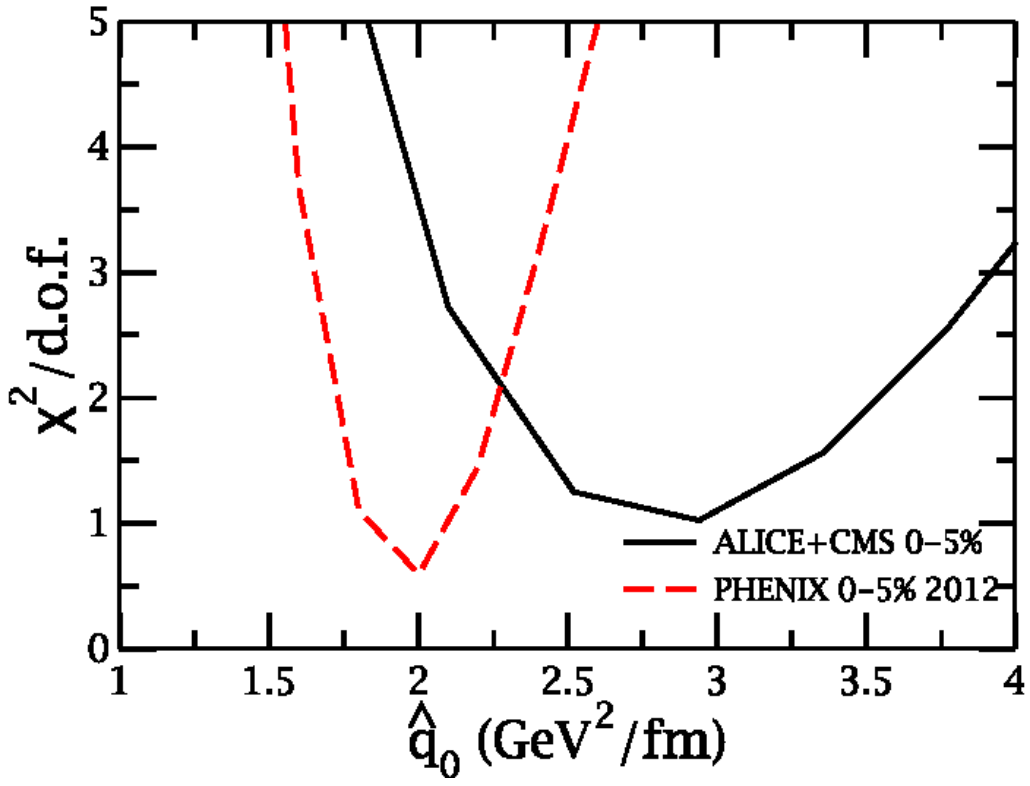

FIGURE 3: χ^2 d.o.f. Fitting of PHENIX, ALICE, and CMS Data

Above is the χ^2/d.o.f presentation of the best fit values for $\hat{q}$. $\chi 2$ is presented as a function of $\hat{q}_0$, the initial gluon jet transport parameter. Fits were made by fitting HT model calculations of $R_{AA}(p_T)$ (shown in Figures 1 and 2) to PHENIX (RHIC) data [75, 76] and data sets from ALICE [25] and CMS [24] (LHC) combined. The best fits shown in the two previous figures (Figures 1 and 2) is verified by the χ^2 calculation, and are at $\hat{q}_0 \approx 2.0$ GeV^2/fm for RHIC, and $\hat{q}_0 \approx 2.9$ GeV^2/fm for the LHC.

To appropriately compare medium properties, I will only consider the value of $\hat{q}$ directly extracted by the HT model using constraints on the model parameters as provided by the experimental data. This will allow for a more accurate comparison to phenomenological jet quenching studies. To do this, I will consider only the suppression factor for single inclusive hadron spectra ($R_{AA}(p_T)$) at RHIC and the LHC. The jet transport coefficient $\hat{q}$ should be a function of both local temperature and jet energy within the HT model, and jet energy will vary with jet propagation length. The value of $\hat{q}$ for a quark jet at the center of 0-5% Au+Au and Pb+Pb collisions will be used as a gauge of medium properties. This will be done at the maximum density achieved in the previously mentioned heavy ion collisions, and will be applied to the bulk evolution when the hydroynamic models are at initial time τ_0 = 0.6fm/c. The intital temperatures for the hydrodynamic model will be set at T_0=346-373 MeV (RHIC) and T_0 = 447-486 MeV (LHC), where these most central (0-5%) collisions of Au+Au and Pb+Pb will be at $\sqrt{s}$ = 200 GeV/n at RHIC and Pb+Pb collisions at $\sqrt{s}$ = 2.76 TeV/n at LHC, respectively.

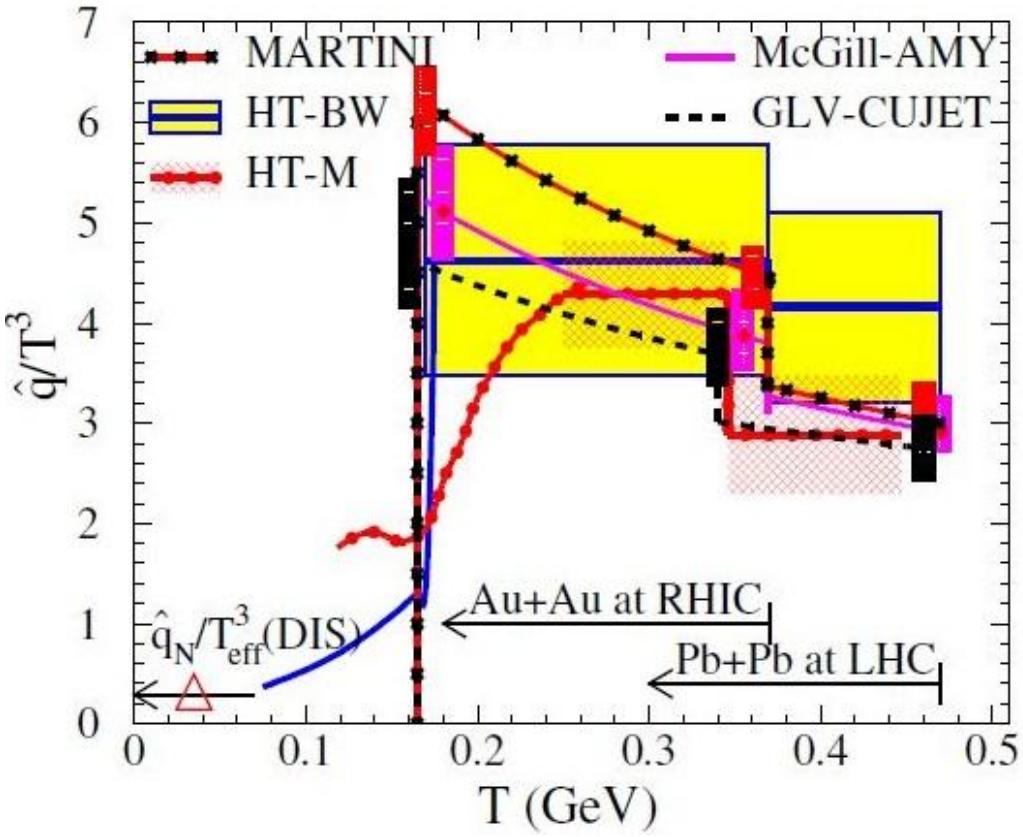

FIGURE 4: Comparative Results of Five Different Approaches to Energy Loss

Figure 4 presents assumed temperature dependent results of the jet transport coefficient scaled as $\hat{q}/T^3$ for 5 different models. The red dotted line represents the calculations for this thesis. At initial time τ_0 = 0.6 fm/c in 0-5% centrality A+A (Au+Au and Pb+Pb) collisions, values of $\hat{q}$ are extracted from fitting in both the HT-M and HT-BW. This fitting was done using a comparison of calculated values with experimental data from RHIC and the LHC for R_{AA}. For GLV-CUJET, MARTINI, and McGill-AMY, values of $\hat{q}$ are calculated within each model using experimentally constrained parameters (RHIC and LHC data). The quark jet considered has initial E=10 GeV [77]. The filled boxes are errors at three separate temperatures at RHIC and the LHC, while the ranges of temperatures are indicated by arrows. Finally, DIS experiments are included and noted by the triangle, which indicates the value of $\hat{q}_N/T_{eff}^3$ in cold nuclei.

Figure 4 shows the results I obtained as they compare to results of other models within the JET Collaboration. The jet transport coefficient $\hat{q}$ for a quark jet is either extracted (HT-M, HT-BW) or calculated (GLV-CUJET, MARTINI, McGill-AMY) as a function of initial temperature at initial energy E=10 GeV [77]. Initial values for $\hat{q}$ (assumed to be independent of energy in the HT model) are are $\hat{q}_0$ =0.89 ± 0.11 GeV^2/fm in the center of 0-5% Au+Au collisions at RHIC, and $\hat{q}_0$ =1.29 ± 0.27 GeV^2/fm in 0-5% Pb+Pb collisions at LHC (note: these values are for quark jets, and are 4/9 the values of those for gluon jets, which are those in the above figures). An assumption in the HT model is that $\hat{q}$ is assumed to follow the entropy density, and therefore $\hat{q}$/T^3 (Figure 4) is calculated based using the parameterized EOS [79] within the hydrodynamic evolution of the bulk medium, for temperatures close to and below the QCD phase transitions.

Variation between models of the $\hat{q}$/T^3 values in Figure 4 are considered to be theoretical uncertainties. The wide range of values, which have been constrained by the measured suppression factors for single hadron spectra at RHIC and LHC, have been extracted as follows:

$$\frac{\hat{q}}{T^3} \approx \begin{cases} 4.6 \pm 1.2 & \text{at RHIC,} \\ 3.7 \pm 1.4 & \text{at LHC.} \end{cases} \qquad (7)$$

These values are for the highest temperatures reached in 0-5% centrality Au+Au collisions at RHIC and Pb+Pb collisions at LHC. Consistent with leading order (LO) pQCD correction [80] estimates, these values are very close to an earlier estimate [6]. They do however, present a surprisingly small value for the strong coupling constant.

Values of $\hat{q}_N$/T$_{eff}$ from jet quenching in DIS [79] of cold nuclei are also included in Figure 4. For an ideal quark gas with 3 quarks within each nucleon in a large nucleus, the value of $\hat{q}_N$ = 0.02-0.06 GeV^2/fm at an effective temperature was used, and the result is an order of magnitude smaller than in Au+Au collisions at RHIC and Pb+Pb collisions at the LHC.

CHAPTER 5: CONCLUSIONS AND OUTLOOK

For this thesis, I conducted a study on the jet transport parameter and extracted jet parameters applicable to parton energy loss. This energy loss, due to jet interactions within a dense medium, has parameters constrained by experimental data from RHIC and the LHC, and is for suppression factors relating to large transverse momentum hadron spectra in high energy heavy ion collisions. A deeper understanding of the temperature dependence of $\hat{q}$ within the HT parton energy loss model have been made possible due to new data from the LHC, combined with data from RHIC and advances in our understanding and modeling of jet quenching and bulk evolution. These new constraints to the assumed temperature dependence of $\hat{q}$ and its implementation have allowed for significant narrowing of the acceptable variation of $\hat{q}$ extracted, as compared to earlier efforts [57, 58]. This updated extracted value is consistent with pQCD as well as (next to leading order) NLO anti-de Sitter/conformal field theory (AdS/CFT SYM) results. A first investigation of jet energy and jet transport coefficient temperature dependence was made possible by the use of a large range of p_T results from the experimental data and higher temperatures reached in the center of heavy ion collisions at the LHC.

From this point, there are many other studies possible using hard probes constrained by experimental data. This first step has proved the effectiveness of this method, and can be extended to a range of other observables including dihadron and gamma-hadron correlations, single jets, dijets and gamma-jets suppressions, azimuthal asymmetries, modification of jet profile and jet fragmentation functions. To do this, the studies should be done using a realistic model for jet quenching. This model should be inclusive of hadronization and bulk evolution which should be constrained by experimental data for bulk hadron spectra. A full Monte Carlo

simulation that involves an evolving jet shower in expanding medium is required to do this. Uncertainties in jet transport parameters can be further reduced from advances in theoretical understanding of jet quenching and modeling of bulk evolution, complementary statistical data from RHIC and the LHC, and greater precision in measurements. Through achieving this, we should also achieve a quantitative description and understanding of the QGP.

Current results have been summarized in Figure 4. The JET Collaboration includes other models that investigate parton energy loss in addition to the HT-M model that I used for my calculations: GLV-CUJET, McGill-AMY, MARTINI, and HT-BW. A wider range of jet energies and maximum temperatures in 0-5% centrality A+A collisions to establish a full quantitative spectrum for the jet transport parameter $\hat{q}$(E,T). Lower energy ($\sqrt{s}$ = 0.02 - 0.2 TeV/n) experimental data from RHIC and higher energy ($\sqrt{s}$ = 5.5 TeV/n) data from the LHC on nuclear modification factors will enable greater constraint on jet-medium interactions. Both constraints imposed by bulk observables on viscous hydrodynamic calculation and jet quenching calculations for light and heavy quarks jets will be required. One last important and challenging problem still open is reconciliation of bulk "flow" moments with high p_T jet azimuthal multipole moments (v_n). These phenomena occur in the ranges of p_T < 4 GeV/c and p_T > 10 GeV/c, respectively. Finally, perturbative (NLO pQCD) and non-perturbative (lattice QCD and AdS/CFT) methods must be used concurrently to improve theoretical calculations of the jet transport coefficient. This can be done within the broad energy and temperature ranges available at RHIC and the LHC to reduce modeling uncertainties in jet quenching studies.

REFERENCES

[1] J.D. Bjorken: "Energy Loss Of Energetic Partons In Quark - Gluon Plasma: Possible Extinction Of High P(T) Jets In Hadron - Hadron Collisions", FERMILAB-PUB-82-059-THY, 1982.

[2] M. Gyulassy and M. Plumer: "Jet Quenching In Dense Matter", Phys. Lett. B **243**, 432 (1990).

[3] X. N. Wang and M. Gyulassy: "Gluon shadowing and jet quenching in A + A collisions at $\sqrt{s}$ = 200-GeV", Phys. Rev. Lett. **68**, 1480 (1992).

[4] M. Gyulassy and X. N. Wang: "Multiple collisions and induced gluon Bremsstrahlung in QCD", Nucl. Phys. B **420**, 583 (1994).

[5] R. Baier, Y. L. Dokshitzer, S. Peigne and D. Schiff: "Induced gluon radiation in a QCD medium", Phys. Lett. B **345**, 277 (1995).

[6] R. Baier, Y. L. Dokshitzer, A. H. Mueller, S. Peigne and D. Schiff: "Radiative energy loss and p_T-broadening of high energy partons in nuclei", Nucl. Phys. B **484**, 265 (1997).

[7] B. G. Zakharov: "Fully quantum treatment of the Landau-Pomeranchuk-Migdal effect in QED and QCD", JETP Lett. **63**, 952 (1996).

[8] M. Gyulassy, P. Levai and I. Vitev: "Non-Abelian energy loss at finite opacity", Phys. Rev. Lett. **85**, 5535 (2000).

[9] M. Gyulassy, P. Levai and I. Vitev: "Reaction operator approach to non-Abelian energy loss", Nucl. Phys. B **594**, 371 (2001).

[10] U. A. Wiedemann: "Gluon radiation off hard quarks in a nuclear environment: Opacity expansion", Nucl. Phys. B **588**, 303 (2000).

[11] U. A. Wiedemann: "Jet quenching versus jet enhancement: A quantitative study of the BDMPS-Z gluon radiation spectrum", Nucl. Phys. A **690**, 731 (2001).

[12] X. F. Guo and X. N. Wang: "Multiple Scattering, Parton Energy Loss and Modified Fragmentation Functions in Deeply Inelastic eA Scattering", Phys. Rev. Lett. **85**, 3591 (2000).

[13] X. N. Wang and X. F. Guo: "Multiple parton scattering in nuclei: Parton energy loss", Nucl. Phys. A **696**, 788 (2001).

[14] P. Arnold, G. D. Moore and L. G. Yaffe: "Photon emission from ultrarelativistic plasmas", JHEP **0111**, 057 (2001).

[15] P. Arnold, G. D. Moore and L. G. Yaffe: "Photon and Gluon Emission in Relativistic Plasmas", JHEP **0206**, 030 (2002).

[16] X. N. Wang: "Systematic study of high p_T hadron spectra in p-p, p-A and A-A collisions from SPS to RHIC energies", Phys. Rev. C **61**, 064910 (2000).

[17] M. Gyulassy, I. Vitev and X. N. Wang: "High p_T azimuthal asymmetry in noncentral A + A at RHIC", Phys. Rev. Lett. **86**, 2537 (2001).

[18] J. Adams *et al.* [STAR Collaboration]: "Evidence from d + Au measurements for final-state suppression of high p_T hadrons in Au + Au collisions at RHIC", Phys. Rev. Lett. **91**, 072304 (2003); "Transverse momentum and collision energy dependence of high p_T hadron suppression in Au + Au collisions at ultra-relativistic energies", Phys. Rev. Lett. **91**, 172302 (2003).

[19] S. S. Adler *et al*. [PHENIX Collaboration]: "Suppressed π^0 production at large transverse momentum in central Au+Au collisions at $\sqrt{s_{NN}}$ = 200-GeV", Phys. Rev. Lett. **91**, 072301 (2003).

[20] C. Adler *et al*.: "Disappearance of back-to-back high p_T hadron correlations in central Au+Au collisions at $\sqrt{s_{NN}}$= 200-GeV",Phys. Rev. Lett. **90**, 082302 (2003).

[21] X.-N. Wang, Z. Huang, I. Sarcevic: "Jet quenching in the opposite direction of a tagged photon in high-energy heavy ion collisions", Phys. Rev. Lett. **77**, 231-234 (1996) [hep-ph/9605213].

[22] A. Adare *et al*. [PHENIX Collaboration]: "Photon-Hadron Jet Correlations in p+p and Au+Au Collisions at $\sqrt{s_{NN}}$ = 200 GeV", Phys. Rev. C **80**, 024908 (2009) [arXiv:0903.3399 [nucl-ex]].

[23] B. I. Abelev *et al*. [STAR Collaboration]: "Studying Parton Energy Loss in Heavy-Ion Collisions via Direct-Photon and Charged-Particle Azimuthal Correlations", Phys. Rev. C **82**, 034909 (2010) [arXiv:0912.1871 [nucl-ex]].

[24] S. Chatrchyan *et al*. [CMS Collaboration]: "Study of high-p_T charged particle suppression in Pb-Pb compared to p-p collisions at $\sqrt{s_{NN}}$ = 2.76 TeV", Eur. Phys. J. C **72**, 1945 (2012) [arXiv:1202.2554 [nucl-ex]].

[25] B. Abelev *et al*. [ALICE Collaboration]: "Centrality Dependence of Charged Particle Production at Large Transverse Momentum in Pb-Pb Collisions at $\sqrt{s_{NN}}$ = 2.76 TeV", Phys. Lett. B **720**, 52 (2013) [arXiv:1208.2711 [hep-ex]].

[26] K. Aamodt *et al*. [ALICE Collaboration]: "Particle-yield modification in jet-like azimuthal di-hadron correlations in Pb-Pb collisions at $\sqrt{s_{NN}}$ = 2.76 TeV", Phys. Rev. Lett. **108**, 092301 (2012) [arXiv:1110.0121 [nucl-ex]].

[27] I. Vitev and B.-W. Zhang: "Jet tomography of high-energy nucleus-nucleus collisions at next-to-leading order", Phys. Rev. Lett. **104**, 132001 (2010).

[28] G. Aad *et al*. [ATLAS Collaboration]: "Measurement of the jet radius and transverse momentum dependence of inclusive jet suppression in lead-lead collisions at $\sqrt{s_{NN}}$ = 2.76 TeV with the ATLAS detector", Phys. Lett. B **719**, 220 (2013) [arXiv:1208.1967 [hep-ex]].

[29] G. Aad *et al*. [ATLAS Collaboration]: "Measurement of the Azimuthal Angle Dependence of Inclusive Jet Yields in Pb+Pb Collisions at $\sqrt{s_{NN}}$ = 2.76 TeV with the ATLAS detector", [arXiv:1306.6469 [hep-ex]].

[30] G. Aad *et al*. [Atlas Collaboration]: "Observation of a Centrality-Dependent Dijet Asymmetry in Lead-Lead Collisions at $\sqrt{s_{NN}}$ = 2.77 TeV with the ATLAS Detector at the LHC", Phys. Rev. Lett. **105**, 252303 (2010).

[31] S. Chatrchyan *et al*. [CMS Collaboration]: "Jet momentum dependence of jet quenching in Pb-Pb collisions at $\sqrt{s_{NN}}$ = 2.76 TeV", Phys. Lett. B **712** (2012) 176 [arXiv:1202.5022 [nucl-ex]].

[32] CMS Collaboration: "Studies of jet quenching using isolated-photon+jet correlations in Pb-Pb and p-p collisions at $\sqrt{s_{NN}}$ = 2.76 TeV", Phys. Lett. B **718**, 773 (2012).

[33] ATLAS Collaboration: "Measurement of the correlation of jets with high p_T isolated prompt photons in lead-lead collisions at $\sqrt{s_{NN}}$ =2.76 TeV with the ATLAS detector at the LHC", Report No. ATLAS-CONF-2012-121.

[34] X.-N. Wang: "Discovery of jet quenching and beyond", Nucl. Phys. **A750**, 98-120 (2005). [nucl-th/0405017].

[35] I. Vitev and M. Gyulassy: "High p_T tomography of d+Au and Au+Au at SPS, RHIC, and LHC", Phys. Rev. Lett. **89**, 252301 (2002).

[36] X.-N. Wang: "High p_T Hadron Spectra, Azimuthal Anisotropy and Back-to-Back Correlations in High-energy Heavy-ion Collisions", Phys. Lett. B **595**}, 165 (2004) [arXiv:nucl-th/0305010].

[37] K. J. Eskola, H. Honkanen, C. A. Salgado and U. A. Wiedemann: "The fragility of high-p_T hadron spectra as a hard probe", Nucl. Phys. A **747**}, 511 (2005).

[38] T. Renk: "Through the blackness: High p_T hadrons probing the central region of 200-AGeV Au-Au collisions", Phys. Rev. C **74**, 024903 (2006).

[39] H. Zhang, J. F. Owens, E. Wang and X.-N. Wang: "Dihadron Tomography of High-Energy Nuclear Collisions in NLO pQCD", Phys. Rev. Lett. **98**, 212301 (2007).

[40] G. Y. Qin, J. Ruppert, C. Gale, S. Jeon, G. D. Moore and M. G. Mustafa: "Radiative and Collisional Jet Energy Loss in the Quark-Gluon Plasma at RHIC", Phys. Rev. Lett. **100**, 072301 (2008) [arXiv:0710.0605 [hep-ph]].

[41] T.~Renk: "Towards jet tomography: gamma-hadron correlations", Phys. Rev. C **74**, 034906 (2006) [hep-ph/0607166].

[42] H. Zhang, J. F. Owens, E. Wang and X.-N. Wang: "Tomography of high-energy nuclear collisions with photon-hadron correlations", Phys. Rev. Lett. **103**, 032302 (2009) [arXiv:0902.4000 [nucl-th]].

[43] G. Y. Qin, J. Ruppert, C. Gale, S. Jeon and G. D. Moore: "Jet energy loss, photon production, and photon-hadron correlations at RHIC", Phys. Rev. C **80**, 054909 (2009) [arXiv:0906.3280 [hep-ph]].

[44] M. Gyulassy, I. Vitev, X.-N. Wang *et al.*: "Jet quenching and radiative energy loss in dense nuclear matter", In *Hwa, R.C. (ed.) et al.: Quark gluon plasma* 123-191 [nucl-th/0302077].

[45] A. Kovner, U. A. Wiedemann: "Gluon radiation and parton energy loss", In *Hwa, R.C. (ed.) et al.: Quark gluon plasma* 192-248 [hep-ph/0304151].

[46] A. Majumder and M. Van Leeuwen: "The Theory and Phenomenology of Perturbative QCD Based Jet Quenching", Prog. Part. Nucl. Phys. A **66**, 41 (2011) [arXiv:1002.2206 [hep-ph]].

[47] N. Armesto, B. Cole, C. Gale, W. A. Horowitz, P. Jacobs, S. Jeon, M. van Leeuwen and A. Majumder *et al*: "Comparison of Jet Quenching Formalisms for a Quark-Gluon Plasma 'Brick'", Phys. Rev. C **86**, 064904 (2012) [arXiv:1106.1106 [hep-ph]].

[48] X.-F. Chen, T. Hirano, E. Wang, X.-N. Wang and H. Zhang: "Suppression of high p_T hadrons in Pb+Pb Collisions at LHC", Phys. Rev. C **84**, 034902 (2011) [arXiv:1102.5614 [nucl-th]].

[49] A. Majumder and C~Shen: "Suppression of the High p_T Charged Hadron R_{AA} at the LHC", Phys. Rev. Lett. **109**, 202301 (2012) [arXiv:1103.0809 [hep-ph]].

[50] K. C. Zapp, F. Krauss and U. A.Wiedemann: "A perturbative framework for jet quenching", JHEP **1303**, 080 (2013) [arXiv:1212.1599 [hep-ph]].

[51] T. Renk: "The Physics probed by the p_T Dependence of the Nuclear Suppression Factor", Phys. Rev. C **88**, 014905 (2013) [arXiv:1302.3710 [hep-ph]].

[52] X.-F. Chen, C. Greiner, E. Wang, X.-N. Wang and Z. Xu: "Bulk matter evolution and extraction of jet transport parameter in heavy-ion collisions at RHIC", Phys. Rev. **C81**, 064908 (2010) [arXiv:1002.1165 [nucl-th]].

[53] S. A. Bass, C. Gale, A. Majumder, C. Nonaka, G. Y. Qin, T. Renk and J. Ruppert: "Systematic Comparison of Jet Energy-Loss Schemes in a realistic hydrodynamic medium", Phys. Rev. C **79**, 024901 (2009).

[54] N. Armesto, M. Cacciari, T. Hirano, J. L. Nagle and C. A. Salgado: "Constraint fitting of experimental data with a jet quenching model embedded in a hydrodynamical bulk medium", [arXiv:0907.0667 [hep-ph].

[55] H. Song and U. W. Heinz: "Suppression of elliptic flow in a minimally viscous quark-gluon plasma", Phys. Lett. B **658**, 279 (2008) [arXiv:0709.0742 [nucl-th]].

[56] H. Song and U. W. Heinz: "Causal viscous hydrodynamics in 2+1 dimensions for relativistic heavy-ion collisions", Phys. Rev. C **77**, 064901 (2008) [arXiv:0712.3715 [nucl-th]].

[57] Z. Qiu, C. Shen and U. Heinz: "Hydrodynamic elliptic and triangular flow in Pb-Pb collisions at $\sqrt{s}$ = 2.76ATeV", Phys. Lett. B **707**, 151 (2012) [arXiv:1110.3033 [nucl-th]].

[58] Z. Qiu and U. Heinz: "Hydrodynamic event-plane correlations in Pb+Pb collisions at $\sqrt{s}$ = 2.76 TeV", Phys. Lett. B **717**, 261 (2012).

[59] A. Das and T. Ferbel: "Introduction to Nuclear and Particle Physics" 2nd edition, World Scientific Singapore, 2003.

[60] M. Gell-Man, Y. Ne'eman: "The Eightfold Way", Westview Press Boulder CO, 2000.

[61] K. Krane: "Introductory Nuclear Physics", Wiley Canada, 1988.

[62] R Dunlap: "The Physics of Nuclei and Particles", Brooks/Cole, Canada, 2004.

[63] M. K. Sundaresan: "Handbook of Particle Physics", CRC Press, Boca Raton, FL, 2001.

[64] A. Majumder: "Jet modification in the next decade: a pedestrian outlook", Pramana

[65] R. Baier and Y. Mehtar-Tani:"Jet quenching and broadening: the transport coefficient $\hat{q}$ in an isotropic plasma", Phys.Rev.C**78**:064906 (2008) [arXiv:0806.0954v1].

[66] R. J. Fries: "Higher twist effects in nuclei", [arXiv:hep-ph/0201311v1].

[67] A.~Majumder: "Hard collinear gluon radiation and multiple scattering in a medium", Phys. Rev. D **85**, 014023 (2012) [arXiv:0912.2987 [nucl-th]].

[68] J. C. Collins, D. E. Soper and G. F. Sterman: "Factorization For Short Distance Hadron - Hadron Scattering", Nucl. Phys. B **261**, 104 (1985); **Note that factorization has never been proven in heavy-ion collisions to the same level of rigor as in particle collisions, however see J. W. Qiu and G. F. Sterman, "Power corrections to hadronic scattering. 2. Factorization", Nucl. Phys. B **353**, 137 (1991).

[69] G. Altarelli and G. Parisi: "Asymptotic Freedom in Parton Language", Nucl. Phys. B **126**, 298 (1977).

[70] A. Majumder: "The in-medium scale evolution in jet modification", [arXiv:0901.4516 [nucl-th].

[71] A. Idilbi and A. Majumder: Extending Soft-Collinear-Effective-Theory to describe hard jets in dense QCD media", Phys. Rev. D **80**, 054022 (2009) [arXiv:0808.1087 [hep-ph]].

[72] A. Majumder: "Calculating the jet quenching parameter $\hat{q}$ in lattice gauge theory", Phys. Rev. C **87**, no. 3, 034905 (2013) [arXiv:1202.5295 [nucl-th]].

[73] A. Majumder, C. Nonaka and S. A. Bass: "Jet modification in three dimensional fluid dynamics at next-to-leading twist", Phys. Rev. C **76**, 041902 (2007) [nucl-th/0703019].

[74] C. Shen, U. Heinz, P. Huovinen and H. Song: "Systematic parameter study of hadron spectra and elliptic flow from viscous hydrodynamic simulations of Au+Au collisions at $\sqrt{s_{NN}}$ = 200 GeV", Phys. Rev. C **82** 054904 (2010) [arXiv:1010.1856 [nucl-th]].

[75] C. Shen, U. Heinz, P. Huovinen and H. Song: "Radial and elliptic flow in Pb+Pb collisions at the Large Hadron Collider from viscous hydrodynamic", Phys. Rev. C **84**, 044903 (2011) [arXiv:1105.3226 [nucl-th]].

[76] A. Adare *et al*. [PHENIX Collaboration]: "Neutral pion production with respect to centrality and reaction plane in Au+Au collisions at $\sqrt{s_{NN}}$ = 200 GeV", [arXiv:1208.2254 [nucl-ex]].

[77] K. Burke, A. Buzzatti, N. Chang, C. Gale, M. Gyulassy, U. Heintz, S. Jeon, A. Majumder, B. Muller, G.Y. Qin, B. Schenke, C Shen, X.N. Wang, J. Xu, C. Young, H. Zhang [JET Collaboration]: "Extracting jet transport coefficient from jet quenching at RHIC and LHC", Phys. Rev. C (In Press), [arXiv:1312.5003v2 [nucl-th]] (2013).

[78] P. Huovinen and P. Petreczky: "QCD Equation of State and Hadron Resonance Gas", Nucl. Phys. A **837**, 26 (2010) [arXiv:0912.2541 [hep-ph]].

[79] W. T. Deng and X. N. Wang: "Multiple Parton Scattering in Nuclei: Modified DGLAP Evolution for Fragmentation Functions", Phys. Rev. C **81**, 024902 (2010). [arXiv:0910.3403 [hep-ph]]

[80] P. B. Arnold and W. Xiao: "High energy jet quenching in weakly-coupled quark-gluon plasmas", Phys. Rev. D **78**, 125008 (2008). [arXiv:0810.1026 [hep-ph]]

ABSTRACT

DETERMINATION OF JET TRANSPORT PARAMETERS AND THEIR TEMPERATURE DEPENDENCE IN HEAVY-ION COLLISIONS

by

KAREN MARIE BURKE

August 2014

Advisor: Dr. Abhijit Majumder

Major: Physics

Degree: Master of Science

In the continuing effort to describe properties of the quark-gluon plasma, energy loss is studied through leading order higher twist calculations of high transverse momentum single hadron suppression. Input of several values for the jet transport parameter $\hat{q}$ were used at p_T ranges of ~5-20 GeV at RHIC and ~10-100 GeV at LHC, with collision centrality of 0-5%. The results of the calculations are then compiled and compared with experimental data to determine the best fit value for $\hat{q}$.

AUTOBIOGRAPHICAL STATEMENT

I am a native Michigander with a love for all things science. I chose the path of physics after a time studying chemistry, realizing that physics would give me the knowledge and understanding of the world around me that I sought after.